Smart Grid and Renewable Energy, 2026, 17(9), 245-268
https://www.scirp.org/journal/sgre
ISSN Online: 2151-4844
ISSN Print: 2151-481X

Improving the Reliability of a Looped Conventional Distribution Network through Optimized Geographic Placement of Distributed Photovoltaic Generation

Moussa Ahmat[1,2], Jean Benjamin Bidias[2], Yacoub Nassian Nimir[2,3], Kaoga Dieudonne Kidmo[2], Amir Moungache[4]

[1]Higher Teachers' Training School of Bongor, Bongor, Chad
[2]National Advanced School of Engineering of Maroua, University of Maroua, Maroua, Cameroon
[3]Faculty of Engineering Sciences and Techniques, Polytechnic University of Mongo, Mongo, Chad
[4]Department of Exact and Applied Sciences, University of N'Djamena, N'Djamena, Chad
Email: mahmatmedi444@gmail.com

How to cite this paper: Ahmat, M., Bidias, J.B., Nassian Nimir, Y., Kidmo, K.D. and Moungache, A. (2026) Improving the Reliability of a Looped Conventional Distribution Network through Optimized Geographic Placement of Distributed Photovoltaic Generation. *Smart Grid and Renewable Energy*, **17**, 245-268.
https://doi.org/10.4236/sgre.2026.179012

Received: July 13, 2026
Accepted: September 21, 2026
Published: September 24, 2026

Abstract

Amidst the continuous growth in demand for electrical energy and the need to reduce greenhouse gas emissions, integrating renewable energy sources into electrical distribution networks offers a viable solution for enhancing the technical, economic, and environmental performance of power systems. This article investigates the impact of high-penetration distributed photovoltaic (PV) generation on the reliability of a conventional looped distribution network. The study focuses specifically on optimizing the geographical coordinates of PV installation sites to improve network reliability indices. The primary objective is to assess how optimizing the geographical coordinates of PV sites affects the reliability of the host distribution network. To achieve this, an Improved Particle Swarm Optimization (IPSO) algorithm is employed. The results demonstrate significant gains in reliability indices, showing reductions of 30.80% for SAIFI, 19.03% for CAIDI, 17.03% for EENS, 17.20% for ECOST, and 17.02% for AENS. These results demonstrate that the optimal integration of distributed photovoltaic generation contributes not only to improving the reliability of the electricity grid but also to reducing the operating costs and environmental impact of the power system.

Keywords

Power Distribution, Conventional Grid, Hybrid Grid, Photovoltaic

Generation, Site Location Optimization, Reliability Indices, Improved Particle Swarm Optimization

1. Introduction

In a world experiencing rapid economic growth, electrical energy must play a pivotal role in ensuring the soundness of this expansion. Given that sustainable development relies on sustainable energy and with electricity demand rising almost daily and projected to reach a 43% global increase by 2035 [1], electric power distribution companies must keep pace; otherwise, they risk financial penalties, particularly if they fail to meet minimum quality standards or adhere to established reliability parameters [2].

To effectively meet this demand amidst global warming, policies aimed at reducing Greenhouse Gas (GHG) emissions are driving a transition from fossil fuels to Renewable Energy Sources (RES) [3]. Among RES, solar energy currently stands out as one of the best options for meeting future energy needs, offering advantages over other sources in terms of availability, cost-effectiveness, accessibility, scalability, and energy efficiency [4]. Furthermore, according to reference [1], the deployment of distributed PV systems will boost distribution grid capacity, enhance grid reliability, and mitigate voltage surges. Additionally, consumers with rooftop photovoltaic systems see significant reductions in their electricity bills [5], and the steadily declining cost of photovoltaic modules [6] represents a major benefit for consumers.

The relationship between distributed renewable generation and distribution-system reliability has received increasing attention in recent studies. In particular, the optimal placement of PV generation has been shown to influence network reliability, power losses, voltage performance and the ability of the system to maintain supply during network disturbances [7]-[10]. Reliability assessment frameworks have also increasingly considered the stochastic behavior of renewable generation and operational failures of distribution-system components [8]-[10].

Furthermore, approximately 90% of the reliability issues encountered by customers (served by power utility companies) stem from electric power distribution systems [11].

Given the importance of reliability in an electrical distribution network, extensive research has been conducted to improve this technical aspect using various methods. Sinishaw *et al.* [11] investigated smart grid technology applications, specifically optimal switching device placement, network reconfiguration, and rapid power restoration to address reliability issues in the Bahir Dar power distribution system. Based on the analysis of outage data, the Bata feeder experiences an average of 604 outages per year and an average total outage duration of 712.425 hours per year. Software analysis indicated reductions in reliability indices, specifically SAIFI, SAIDI, CAIDI, and the Average Service Availability Index (ASAI) by 131.1454 interruptions/year, 245.8348 hours/year, 1.875 hours/customer-interruption, and 0.9719 p.u., respectively. Jaleel *et al.* [12] presented a new approach to reliability assessment and estimated the optimal location and capacity of Distributed Generation (DG) units using multi-objective functions aimed at reducing power losses and improving voltage profiles. The results demonstrate that the proposed approach outperforms other methods, achieving a 60.13% reduction in real power losses and an 88.34% improvement in the voltage profile. Additionally, the SAIFI index was minimized by 1.5686%, the EENS (Expected Energy Not Supplied) index by 39.033%, and the AENS (Average Energy Not Supplied per customer served) index by 0.0154%. Durgadevi *et al.* [13] presented a study aimed at improving the reliable operation of the electrical system by using reliability indices calculated via the Modified Salp Swarm Algorithm (MSSA) both before and after the integration of Distributed Generation (DG) into the power system. Based on the results obtained, the reliability indices for this case, namely SAIFI, SAIDI, CAIDI, ASAI, Information System Usage Analysis (AUSSI), Energy Usage Evaluation (EUE), and Energy Usage Evaluation Analysis (AEUE), showed improvements of approximately 12.5%, 4.32%, 7.28%, 1.09%, 4.53%, 12.00%, and 0.19%, respectively. Suyono *et al.* [14] worked on improving the reliability of an electric power distribution system by optimizing the number and location of sectionalizers, utilizing standard distribution system reliability indices (SAIFI, SAIDI, and CAIDI) alongside Ant Colony Optimization (ACO) and Simulated Annealing (SA) methods. The optimal relocation of the network's 16 existing sectionalizers proved effective, reducing reliability indices by up to 43.96% for SAIFI, 45.52% for SAIDI, and 2.8% for CAIDI. Ali Shaik *et al.* [15] investigated how to reconfigure the distribution network and optimally position Distributed Generation (DG) units to reduce power losses and improve the voltage profile. The results indicate that network reconfiguration and DG placement are the best techniques for reducing power losses and managing voltage instability, thereby enhancing overall performance. The power loss index was 0.6984 at half-load and 0.5955 at full-load both lower than previous values while the active power loss index was 0.6899 under overload conditions. The EENS, SAIDI, and SAIFI reliability indices showed improvement compared to the baseline cases. Agajie *et al.* [16] investigated the optimal placement of Distributed Energy Resources (DER) to evaluate the impact of varying levels of Distributed Generation (DG) penetration on system reliability and voltage profiles, while also conducting a detailed analysis of the costs associated with integrating DG units into the distribution system. The calculated results indicate that the integration of DG units improved overall system reliability by 40.55% for SAIFI, 38.04% for SAIDI, 1.53% for CAIDI, 37.76% for EENS, 52.29% for AENS, and 37.76% for ECOST. Sai Kiran *et al.* [17] employed a hybrid (analytical-simulation) method to evaluate the reliability of a microgrid featuring priority loads and distributed renewable energy resources. This approach utilized a mixed-integer optimization model designed to maximize microgrid system reliability by determining the number of critical and non-critical loads that could be served at each time step. The results demonstrated improvements of 29.8% in SAIFI, 12.26% in SAIDI, 2.76% in CAIDI, 85.28% in EENS, and 33.32% in ECOST. Josue *et al.* [18] used a numerical optimization technique to enhance reliability by analyzing load profiles with the aim of mitigating load shedding in Central Africa (Kinshasa). To this end, the study proposed ten strategies for reducing load shedding within the grid: improved load forecasting, grid infrastructure upgrades, load shedding scheduling, demand-side management programs, energy efficiency initiatives, decentralized generation, grid automation and monitoring, consumer education and engagement, policy and regulatory support, and updated load profile analysis. Other recent studies, notably those by Mansaray *et al.* on the integration of decentralized solar PV into the distribution grid of Freetown, Sierra Leone, also illustrate the growing interest in the deployment of photovoltaics within African power systems [19]. Other studies have also demonstrated that distributed photovoltaic generation can contribute to improving the technical performance and reliability of distribution networks when its location and capacity are appropriately determined. However, the stochastic nature of solar generation and its interaction with network operating conditions make the optimal integration of PV resources a challenging planning problem [20].

However, a review of the literature reveals that researchers have not yet investigated the impact of optimizing the geographic coordinates of PV generation sites on the reliability indices of a looped electrical distribution network. The objective of this research is to present a novel reliability improvement method that optimizes the geographic coordinates and output of actual photovoltaic generation sites, simulating power injection into a real-world looped distribution network.

2. Materials and Methods

To demonstrate the effectiveness of the chosen optimization method, we decided to apply it to an actual looped distribution network (that of the city of N'Djamena). Given that the city's power generation is 100% fossil-fuel-based (conventional) [21], and recognizing the need to contribute to global efforts to reduce greenhouse gas emissions, we opted to hybridize this conventional network by simulating the integration of photovoltaic generation sites into the distribution grid.

To do this, we proceeded according to the flowchart (**Figure 1**) below.

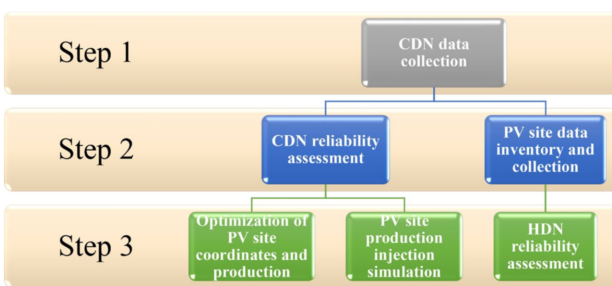

Figure 1. Flowchart outlining the steps for carrying out the activities.

The following hardware (Figure 2) and software (Figures 3-5) were used in the course of this research.

Figure 2. Garmin GPS.

Figure 3. Excel software interface.

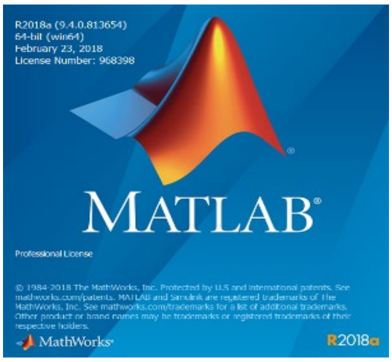

Figure 4. Matlab software interface.

Figure 5. ETAP software interface.

2.1. Description of the Studied Network and Data Used

The data used in this study were obtained from Chad's National Electricity Company (SNE) and pertain to the medium-voltage distribution network of the city of N'Djamena. The observation period covers the year 2023. The collected data include the characteristics of MV feeders and MV/LV transformers, outage histories, power demand figures, the geographical locations of transformers and photovoltaic sites, and the information required to calculate reliability indices.

The studied network section consists of three medium-voltage (15 kV) feeders supplying a total of 90 MV/LV (15/0.4 kV) transformer substations, serving approximately 22,560 customers across various residential, commercial, and administrative areas of N'Djamena. The network features a conventional looped topology that allows for supply restoration operations in the event of a fault.

Reliability assessment is based on operational records from 2023. Failure parameters were derived from actual events observed on the network (outage frequency and duration), assuming a mean time to repair of 12 hours. Network reconfiguration maneuvers are carried out using a mixed switching strategy combining manual operations with existing network switching devices to isolate faulty sections and restore power to healthy sections.

The SAIFI, SAIDI, CAIDI, EENS, ECOST, AENS, and VAENS indices were calculated both before and after the integration of distributed photovoltaic generation to quantitatively assess the impact of the proposed method on distribution network reliability.

2.2. Evaluation of the Conventional Distribution Network (CDN)

Parameters for Evaluating the Reliability of the Conventional Network

This involves evaluating the conventional distribution network by determining, for each feeder:

- Customer-based reliability indices (SAIFI, SAIDI, and CAIDI);
- And energy-based reliability indices (EENS, ECOST, AENS, and VAENS).

1) Determination of customer-based reliability indices

$$\text{SAIFI} = \frac{\text{Total number of customers subject to load shedding}}{\text{Total number of customers served}} = \frac{\sum_{i=1}^{n} \lambda_i N_i}{N} \quad (1)$$

$$\text{SAIDI} = \frac{\text{Total duration of interruptions}}{\text{Total number of customers served}} = \frac{\sum_{i=1}^{n} U_i N_i}{N} \quad (2)$$

$$\text{CAIDI} = \frac{\text{Total duration of interruptions}}{\text{Total number of customers subject to load shedding}} = \frac{\sum_{i=1}^{n} U_i N_i}{\sum_{i=1}^{n} \lambda_i N_i} = \frac{\text{SAIDI}}{\text{SAIFI}} \quad (3)$$

where n = total number of load points, λ_i = average failure rate of each segment i, N_i = number of customers shed at the i^{th} node, and N = total number of customers served.

2) Determination of energy-based reliability indices

$$\text{EENS} = U_i \sum La(i) \tag{4}$$

$$\text{AENS} = \frac{\text{Total energy not supplied}}{\text{Total number of customers served}} = \frac{\sum U_i La(i)}{\sum N_i} \tag{5}$$

$$\text{ECOST} = \sum (P \cdot C \cdot H) \tag{6}$$

where U_i is the annual outage duration for load point i, La is the average load at each load point busbar, P is the received active power, C is the cost of the received active power, and H is the duration or period (in hours) of the received active power availability.

2.3. Optimization Method for Photovoltaic Production Site Coordinates

A wide range of optimization techniques has been investigated for the optimal allocation of distributed generation, including genetic algorithms, mathematical programming and particle-swarm-based methods. Recent studies have also employed improved or hybrid metaheuristic algorithms to determine the optimal location and sizing of renewable distributed generation while satisfying technical and reliability constraints [22]-[25].

In this study, an Improved Particle Swarm Optimization algorithm (IPSO) is therefore proposed. The objective is to optimize the position (x, y coordinates) of each production site relative to the position of the corresponding transformer substation while simultaneously maximizing production to meet local consumption needs as well as a significant portion of the demand in the area supplied by that same transformer. To achieve this, an improved Particle Swarm Optimization algorithm (IPSO) is used as follows:

Let $X(x_i, y_i)$ be the coordinates of any given physical site (where x_i is the longitude and y_i is the latitude of site i); the IPSO initiates the optimization process using the initial positions of the PV production sites.

$$X_0^k(i,j) = Lb(i,j) + rand\left(Ub(i,j) - Lb(i,j)\right) \tag{7}$$

X_0^k : initial coordinate of a PV production site.

The determination of PV production site locations proceeds in two stages:

- Stage 1: Determining the production location based on energy demand and the capacities and locations of MV/LV substations in the zone. The search process yields the optimal production site location, Pbest;
- Stage 2: Determining the production location for a neighboring zone, based on the capacities and locations of MV/LV substations. The search process yields the optimal location for the neighboring production site, Lbest; this continues until the optimal site locations for the entire distribution network, Gbest, are determined.

The principles governing changes in velocity and position are defined as follows:

$$V_i^{k+1} = \omega \cdot V_i^k + C_1 \cdot rand_1 \left(Pbest - \left(x_i^k + y_i^k \right) \right) + C_2 \cdot rand_2 \left(Gbest - \left(x_i^k + y_i^k \right) \right) \quad (8)$$

$$\left(x_i^{k+1} + y_i^{k+1} \right) = \left(x_i^k + y_i^k \right) + V_i^{k+1} \quad (9)$$

where ω is the weighting function; C_1 and C_2 are the weighting factors; $rand_1$ and $rand_2$ are two uniformly distributed random numbers generated independently between 0 and 1; V_i^k and V_i^{k+1} are the particle velocities at iterations k and $k+1$, respectively; and (x_i^k, x_i^{k+1}) and (y_i^k, y_i^{k+1}) are the longitude and latitude of site i at iterations k and $k+1$, respectively.

The weighting function is given by the equation:

$$\omega = \omega_{max} - \frac{\omega_{max} - \omega_{min}}{itermax} \cdot iter \quad (10)$$

where: ω_{max} = initial weight, ω_{min} = final weight, $itermax$ = maximum number of iterations, and $iter$ = current iteration.

The following table (Table 1) presents the principal parameters of the proposed IPSO algorithm.

Table 1. Parameters of the proposed IPSO algorithm.

Parameter	Value
Swarm size	50 particles
Maximum number of iterations	100
Inertia weight ω	0.7 (constant)
Cognitive coefficient C_1	1.5
Social coefficient C_2	2.0
Number of independent runs	15
Constraint handling	Boundary projection (particles exceeding the search domain are returned to the admissible boundary)
Stopping criterion	Maximum number of iterations reached
Optimized variables	PV site coordinates and PV capacities

The proposed IPSO algorithm was implemented using a swarm of 50 particles and a maximum of 100 iterations. A constant inertia weight of 0.7 was selected based on preliminary numerical tests to provide a suitable balance between global exploration and local exploitation during the optimization process. The cognitive and social learning coefficients were fixed at 1.5 and 2.0, respectively. Since PSO is inherently stochastic, the optimization was independently executed 15 times, and the solution with the best objective function value was retained. The search constraints were enforced using a boundary projection strategy: whenever a particle exceeded the admissible search domain, its position was projected back onto the corresponding boundary. This implementation was specifically configured for the simultaneous optimization of the geographical coordinates and capacities of the distributed photovoltaic sites.

2.3.1. Conceptual Diagram of the Improved PSO Applied to PV Placement

General principle

Each particle in the swarm represents a candidate solution defined by:

- The geographical coordinates of the PV sites (x, y);
- The power injected by each PV site;
- The distribution network transformers have fixed positions, which impose a rigid network topology.

The operating cycle of the IPSO (Improved Particle Swarm Optimization) algorithm can be represented by Figure 6 below.

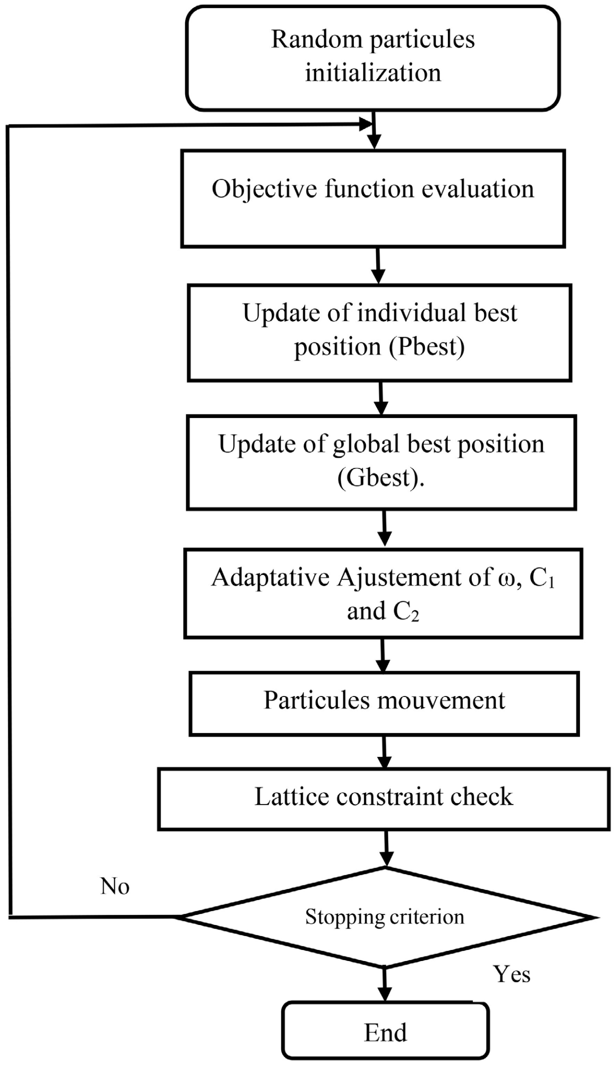

Figure 6. Flowchart of the IPSO algorithm for optimizing the coordinates of PV production sites.

2.3.2. Complete Mathematical Formulation of the Problem

1) Decision variables

The optimization problem aims at determining the optimal geographical coordinates of the photovoltaic sites. The decision vector is defined as

$$X = \left[(Lat_1, Lon_1), (Lat_2, Lon_2), \cdots, (Lat_N, Lon_N)\right] \quad (11)$$

where:

- Lat_i is the latitude of PV site *i*;
- Lon_i is the longitude of PV site *i*;
- $N = 25$ is the number of PV sites considered in this study.

Each particle of the swarm therefore represents a complete geographical configuration of all photovoltaic sites.

2) Objective functions

The objective is to determine an optimal geographical distribution of the photovoltaic sites while maintaining realistic installation locations and improving the electrical performance of the distribution network.

The optimization problem is formulated as

$$J(X) = \alpha \sum_{i=1}^{N} d(PV_i, T_i) + \beta \sum_{i<j} \frac{1}{d(PV_i, PV_j)} + \gamma P(X) \quad (12)$$

where:

$$d(PV_i, T_i) = \sqrt{(Lat_i - Lat_{Ti})^2 + (Lon_i - Lon_{Ti})^2} \quad (13)$$

is the Euclidean distance between the i^{th} photovoltaic site and its associated transformer.

The penalty function is defined as:

$$P(X) = \begin{cases} 0, & \text{if all geographical constraints are satisfied} \\ M, & \text{otherwise} \end{cases}$$

where M is a sufficiently large penalty coefficient

The first term of Equation (12) minimizes the distance between each photovoltaic site and its associated distribution transformer, thereby reducing feeder extension requirements and facilitating local power injection.

The second term of Equation (12) maximizes the geographical dispersion of photovoltaic sites by penalizing excessively close installations, thus preventing unrealistic clustering of generation units.

The third term of Equation (12) represents a penalty function that guarantees feasible geographical solutions.

The weighting coefficients α, β, and γ regulate the relative contribution of each objective component.

Constraints

There are at least four constraints to be met in this optimization: constraints regarding voltage limits, power limits, and transformer capacity limits, as well as constraints concerning the zones authorized for injection into a conventional grid transformer. These constraints are formulated as follows:

Voltage constraints:

$$V_{min} \le V_k \le V_{max}$$

PV power constraints:

$$0 \le P_i \le P_{imax}$$

Transformer capacity constraints:

$$S_{tr} \le S_{trnom}$$

Geographical constraints:

$$(x_i, y_i) \in \text{Permitted zone}$$

2.4. Technical Feasibility of Optimized PV Injection into the Conventional Grid

To efficiently inject power generated at a production site into the conventional distribution grid (following the assessment and optimization of the power produced and the energy demand at each PV site), an intelligent interface system is installed, comprising:

- A pure sine wave inverter sensitive to distribution grid fluctuations;
- An intelligent stabilizer capable of controlling and maintaining the frequency and voltage of both the production site and the grid within acceptable limits;
- An intelligent meter capable of real-time monitoring of energy produced, energy consumed, and energy fed into the grid;
- An intelligent residual-current circuit breaker capable of continuously monitoring the inputs and outputs of the PV injection system regarding both the site and the grid.

The following images (**Figure 7**) show the schematic diagram of the PV injection process:

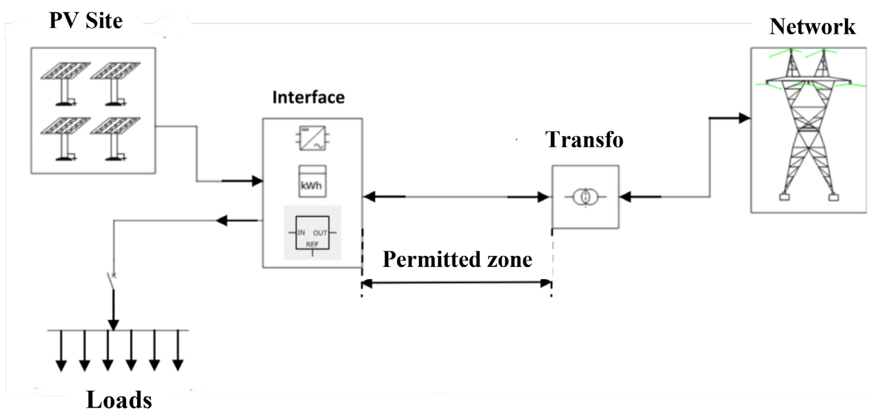

Figure 7. Architecture of photovoltaic grid injection system.

Principle

The DG sources at the PV production site are considered to operate in MPPT mode. They are connected to the load bus via the smart interface system. In a hybrid meshed configuration, when there is insufficient power from the site (e.g., at night) to meet load demands, the smart interface system can draw energy from the Conventional Distribution Network (CDN) via the MV/LV transformer. Conversely, when surplus power is available from the site's DG sources, it can be injected into the CDN grid via the smart interface, the line, and the MV/LV transformer.

The additional constraints to be met during injection, in this instance as well as in other cases cited in the literature [26], are as follows:

- The power flow, P_{ij}, through each branch (i, j) must be less than or equal to the branch's maximum load limit: $P_{ij} \leq P_{chmax}$;
- Power balance constraint: $P_{total}(t) = P_{RDC}(t) + P_{Site}(t)$;
- Converter rating constraint: $(P_{Site}(t))^2 + (Q_{Site}(t))^2 \leq (S_{Site}(t))^2$.

Where P_{total} is the total active power of the CDN, and V_{min} and V_{max} are the minimum and maximum bus voltage magnitude limits set by the grid. P_{Site}, Q_{Site}, and S_{Site} are the active, reactive, and apparent power produced by the PV production site, respectively.

Relationship between IPSO optimization and reliability assessment

It should be emphasized that the IPSO algorithm does not directly minimize the reliability indices. The optimization stage aims at determining the spatial configuration of the distributed PV units by minimizing a weighted objective function combining the PV-to-transformer connection distance and the corresponding integration cost. The resulting optimal PV locations are subsequently introduced into the distribution-network reliability assessment model. The reliability indices, including SAIFI, SAIDI, CAIDI, EENS, AENS and ECOST, are then calculated for the optimized configuration and compared with the reference configuration under identical network, failure-rate, repair-time, load and PV-availability assumptions. Therefore, the reported improvement in reliability represents the effect of the optimized spatial allocation of PV generation, rather than a direct optimization of the reliability indices by IPSO.

2.5. Modeling the Operation of Photovoltaic Systems during Outages

In the simulations performed using ETAP, the output of the photovoltaic installations is assumed to be constant in order to evaluate the impact of photovoltaic site optimization on grid performance under steady-state conditions. Temporal variations in solar irradiance and module temperature were not taken into account in this study.

Each photovoltaic installation is equipped with a smart inverter that ensures normal grid-connected operation while enabling islanded operation when the upstream grid becomes unavailable. When a major fault, such as a short circuit, triggers the opening of protection devices, the faulty section is isolated from the rest of the grid. The inverters then maintain power supply to the local loads connected to their islanded zone, provided that the available photovoltaic power is sufficient.

Given the grid's looped configuration and the adopted protection strategy, no energy injection into other grid sections is permitted during islanded operation. Loads located outside the zone supplied by the photovoltaic installation remain de-energized until the main power supply is restored and the grid returns to its normal configuration. The following table (**Table 2**) presents the key simulation assumptions adopted.

Table 2. Key simulation assumptions.

Parameter	Assumption adopted
PV generation profile	Constant generation
Irradiance variability	Not considered
Normal operating mode	Grid-connected
Operation during a fault	Islanded mode
Inverter type	Smart inverter
Protection behavior	Isolation of the faulted zone
Loads kept energized	Local loads only
Power export to other feeders	Not permitted during islanding

3. Result of the Evaluation of the Conventional Distribution Network (CDN)

The following table (Table 3) presents the evaluation results for the conventional distribution network in the study area.

Table 3. Reliability indices for the conventional distribution network.

No.	The calculated initial parameters of the Conventional Distribution Network (CDN)	The values found in each case
01	System Average Interruption Frequency Index (**SAIFI**, in number of interruptions/customers per year)	**39.34**
02	System Average Interruption Duration Index (**SAIDI**, in hours of interruption per customer per year)	**103.23**
03	Customer Average Interruption Duration Index (**CAIDI** in hours/customers interrupted per year)	**330.72**
04	Expected Energy Not Served (**EENS** in MWh/year)	**55202.45**
05	Cost of Expected Energy Not Supplied (**ECOST** in million dollars/year)	**11.25**
06	Average energy not supplied per customer served (**AENS** in MWh/year)	**2492.93**
07	Average cost of unsupplied energy per customer served (**VAENS** in millions of dollars/year)	**0.52**
08	Average annual interruption frequency experienced by customers in the CDN/Feeder	**160**
09	Average annual outage duration (in hours)	**545.04**

Based on the evaluation results for the conventional distribution network, it is evident that the average interruption frequency index (SAIFI) and the average interruption duration indices (SAIDI and CAIDI) for the network are very high. This indicates that customers on this network frequently experience unplanned outages. Furthermore, the expected energy not supplied and its associated cost (EENS and ECOST), as well as the average energy not supplied per served customer and its cost (AENS and VAENS), are also very high, resulting in significant revenue loss for the energy-producing company.

Given these findings, conducting a study to improve the reliability of this conventional distribution network would be highly beneficial.

4. Results and Discussion

4.1. Optimization of Generation Sites

After carefully applying the optimization methods described above, we obtained optimized coordinates corresponding to the actual site locations. These new site positions were optimized relative to the fixed locations of the transformer substations within the conventional distribution network. The following table (Table 4) presents the results for each PV generation site.

Table 4. Actual and optimized coordinates.

Names of sites and transfers	Measured real (*x*, *y*) coordinates		Optimized (*x*, *y*) coordinates		Fixed (*x*, *y*) coordinates of the transformers	
	Longitudes	Latitudes	Longitudes	Latitudes	Longitudes	Latitudes
A3	15°7'49.55"	12°6'4.07"	15°7'42.64"	12°6'10.55"	15°7'42.82"	12°6'8.03"
A2	15°7'55.63"	12°5'48.23"	15°7'50.74"	12°5'33"	15°7'51.1"	12°5'33.36"
SG	15°8'23.96"	12°5'41.35"	15°8'19.14"	12°5'23.6"	15°8'18.64"	12°5'23.68"
ND1	15°6'13.21"	12°7'18.62"	15°6'10.62"	12°7'17.62"	15°6'10.33"	12°7'17.87"
ND2	15°5'57.16"	12°7'30.58"	15°5'59.46"	12°7'44.15"	15°5'56.58"	12°7'43.87"
ND3	15°5'56.58"	12°7'43.86"	15°5'57.41"	12°7'10.63"	15°6'10.35"	12°7'17.73"
HR	15°5'56.40"	12°7'7.64"	15°6'22.43"	12°8'35.79"	15°5'52.4"	12°7'4.4"
DS	15°6'21.42"	12°8'35.81"	15°6'10.34"	12°7'17.51"	15°6'22.61"	12°8'35.56"
CR	15°4'13.56"	12°7'42.42"	15°5'2.15"	12°6'42.98"	15°5'2.22"	12°6'42.8"
P2	15°4'12.14"	12°7'41.74"	15°4'6.37"	12°7'40.53"	15°4'13.48"	12°7'42.24"
P1	15°6'22.66"	12°8'35.69"	15°4'6.31"	12°7'40.51"	15°4'12.15"	12°7'41.7"
Am1	15°4'16.00"	12°7'30.35"	15°4'16.46"	12°7'29.75"	15°4'16.54"	12°7'34.68"
Am2	15°4'5.00"	12°9'55.34"	15°4'16.5"	12°7'34.79"	15°4'3.25"	12°9'33.52"
PG	15°3'5.98"	12°7'41.27"	15°3'7.74"	12°7'40.55"	15°3'2.6"	12°7'26.14"
Phi	15°3'0.50"	12°7'25.62"	15°3'1.55"	12°7'26.94"	15°2'19.87"	12°6'49.37"
BB	15°4'4.54"	12°5'51.54"	15°5'1.39"	12°5'19.1"	15°3'18.76"	12°7'26.36"
PN	15°2'21.37"	12°6'53.81"	15°2'19.93"	12°6'49.36"	15°3'39.32"	12°5'53.57"
ADj	15°4'4.76"	12°5'51.53"	15°3'56.88"	12°6'17.46"	15°3'32.65"	12°6'14.15"
CD	15°3'38.27"	12°5'58.73"	15°3'39.49"	12°5'53.63"	15°2'19.69"	12°6'49.52"
GM	15°4'5.74"	12°5'49.81"	15°4'4.62"	12°5'51.47"	15°4'10.27"	12°5'31.33"
HBS	15°5'6.79"	12°5'7.25"	15°5'7.33"	12°5'22.74"	15°4'5.8"	12°5'49.78"
NDA	15°4'44.90"	12°5'33.30"	15°3'1.7"	12°7'26.86"	15°4'43.43"	12°5'34.87"
PC1	15°4'23.02"	12°6'16.52"	15°4'23.13"	12°6'16.25"	15°4'33.35"	12°6'52.67"
PC2	15°4'44.99"	12°5'54.68"	15°3'32.73"	12°6'14.28"	15°4'15.71"	12°6'35.32"
PC3	15°4'12.65"	12°6'28.43"	15°4'18.95"	12°6'29.26"	15°4'17"	12°6'30"

4.2. Mapping of Site Locations

We used Excel software to illustrate the locations of actual production sites in relation to the production sites optimized based on the fixed positions of the equivalent transformers. The following (Figure 8) illustrates these locations.

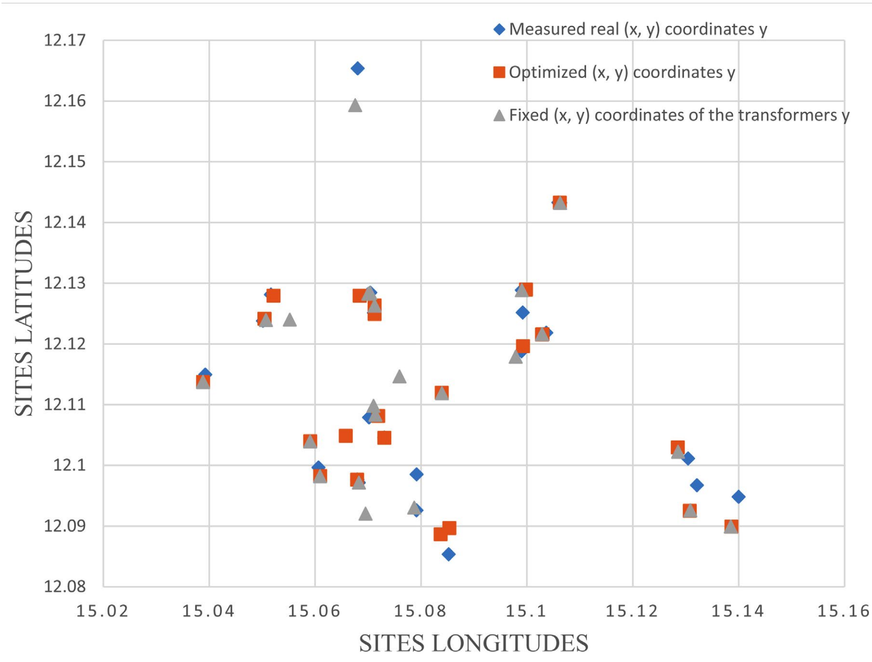

Figure 8. Overview of the coordinates of actual transformer sites and optimized sites, illustrated using Excel software.

4.3. Optimization of Power Output from Generation Sites

To inject generated power effectively and efficiently, it is necessary based on the power demand at each generation site to optimize (specifically, to maximize) the power produced by that site autonomously, while adhering to the grid constraints described in paragraph 2.4 above.

The results obtained after applying the selected optimization method are presented in Table 5 below.

Table 5. Recorded power and optimized power for PV generation sites.

No. of sites	Recorded power outputs (in kW)	Optimized power (in kW)
1	2	5.64
2	3	8.88
3	10	29.8
4	5	15.08
5	5	14.68
6	15	43.42
7	100	285.62

Continued

8	15	45.80
9	75	232.40
10	3	9.41
11	30	95.29
12	3.5	9.99
13	10	29.03
14	6	17.44
15	3.5	10.19
16	4	11.66
17	150	438.22
18	3.5	10.30
19	4.5	13.27
20	3	8.86
21	165	488.79
22	6.5	19.27
23	6	17.80
24	10.5	31.32
25	3.5	10.45

The following Figure 9 shows the power outputs recorded at actual sites compared to the optimized power outputs for each production site.

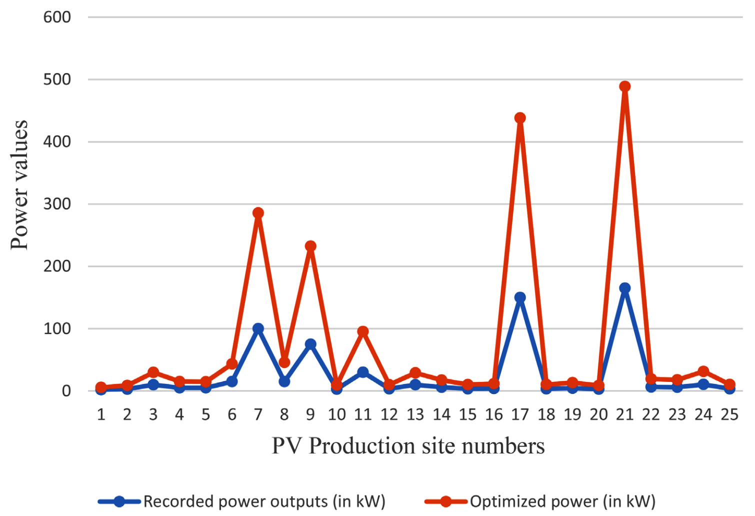

Figure 9. Graph of recorded power levels (red) versus optimized power levels (green).

Figure 9 above shows that the higher the actual power generated, the greater the power obtained after optimization. This is due to the demand at the sites in question, which feature high and varied load concentrations. Regarding Figure 10, a nearly steady increase is observed in the difference between the recorded power and the optimized power as the recorded power levels rise. This indicates a proportional relationship between the power differences and the actual power recorded at each PV generation site.

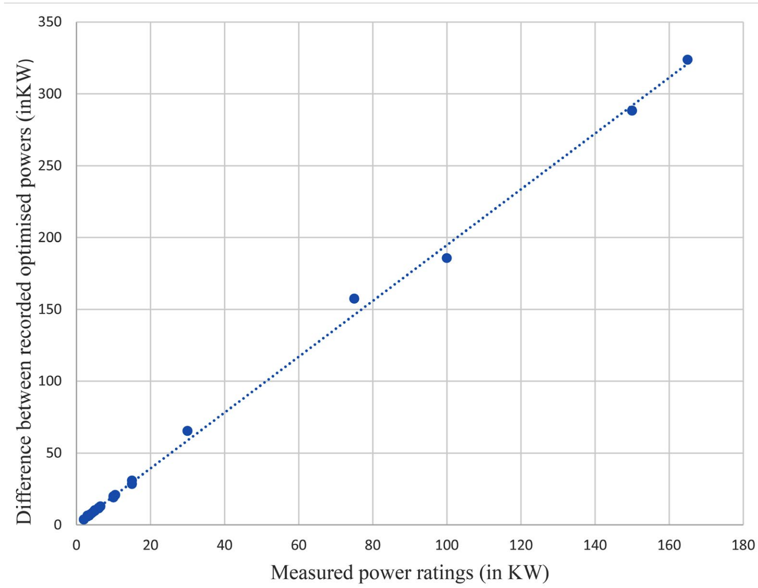

Figure 10. Representation of power deviations as a function of measured power levels.

4.4. Simulation of Power Injection from Distributed PV Sites into the Distribution Grid

After optimizing the locations and output of the photovoltaic generation sites using the Particle Swarm Optimization (PSO) algorithm in MATLAB, we proceeded to inject this power into the study area's conventional distribution grid using ETAP simulation software. This step was taken to verify the effectiveness of the chosen method. The setup diagram for simulating these PV injections is shown in **Figure 11** below.

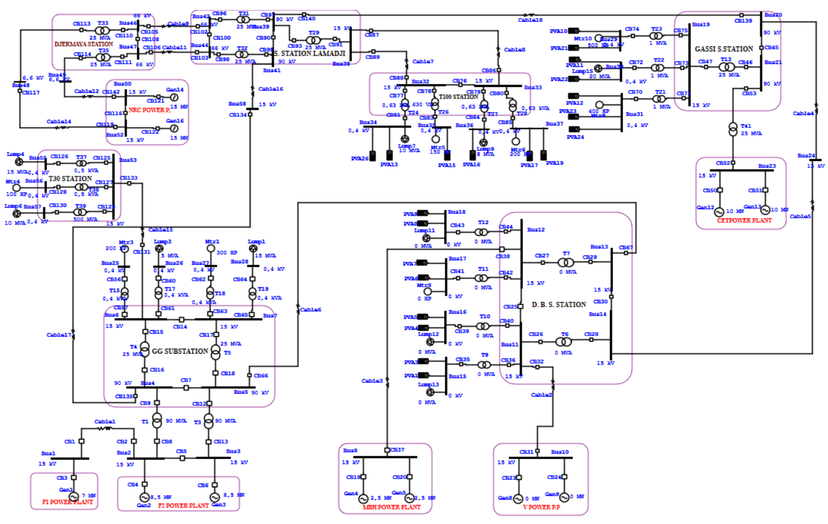

Figure 11. Single-line diagram of the hybrid distribution network.

The results obtained from injecting the photovoltaic output of the 25 production sites are recorded in Table 6 below.

Table 6. Reliability indices.

Indices	Conventional distribution network	Hybrid network before optimization	Hybrid network after optimization
SAIFI (H/customers)	39.34	12.11	8.38
CAIDI (H/customers shed per year)	330.72	19.13	15.49
EENS (MWh/an)	55202.45	7595.21	6302.28
ECOST (million$/an)	11.25	1.57	1.3
AENS (MWh/an)	2492.93	343.05	284.65
VAENS (million$/an)	0.52	0.071	0.059

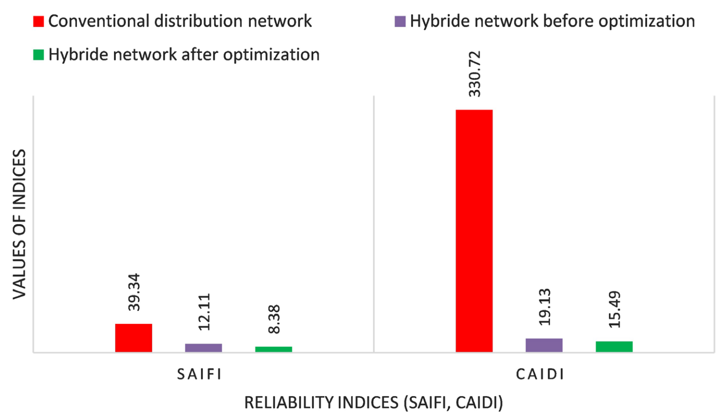

Figure 12. System interruption frequency and customer interruption duration.

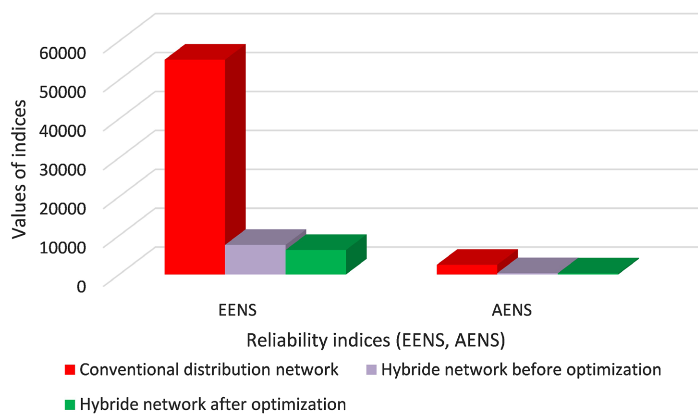

Figure 13. Expected Energy Not Supplied (EENS) and Average Energy Not Supplied per served customer (AENS).

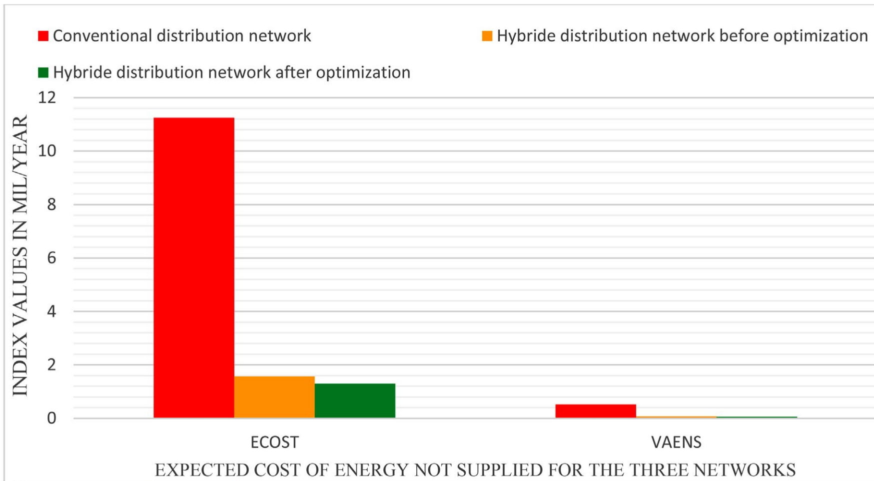

Figure 14. Cost of Expected Energy Not Supplied (ECOST) and Average Energy Not Supplied per Served Customer (VAENS).

When optimized PV generation is injected, a remarkable improvement (reduction) is observed in the System Average Interruption Frequency Index (SAIFI), and a very sharp decrease occurs in the Customer Average Interruption Duration Index (CAIDI) (Figure 12 above). There is also a very sharp decrease in Expected Energy Not Supplied (EENS) and a remarkable decrease in Average Energy Not Supplied per customer (AENS) (Figure 13 above). Furthermore, a very sharp decrease is seen in the Cost of Expected Energy Not Supplied (ECOST), alongside a remarkable improvement in the Cost of Expected Energy Not Supplied per customer (VAENS) (Figure 14 above). The sharp reductions in CAIDI, EENS, and ECOST stem from the fact that outage durations in distribution networks are often long, unlike outage frequencies. Consequently, when injection is performed strategically—targeting residential areas prone to these issues—outage durations improve significantly, explaining these sharp decreases. This indicates that when system interruption duration decreases significantly, the impact on the values of other indices becomes substantial. Moreover, optimizing the locations and power outputs of generation sites leads to further reductions across all indices. This demonstrates that optimizing the coordinates and power outputs of PV sites has a significant impact on the reliability indices of looped hybrid distribution networks.

4.5. Percentage Gains in Reliability Indices

From the preceding Table 4, we derive the percentage improvements for each reliability index when photovoltaic generation site coordinates are optimized and their power outputs are strategically injected into the conventional network. Table 7 below presents the percentage gains for these various reliability indices.

Table 7. Percentage gains in reliability indices.

Reliability indicators	SAIFI	CAIDI	EENS	ECOST	AENS	VAENS
Gain in %	30.80	19.03	17.03	17.20	17.02	17.35

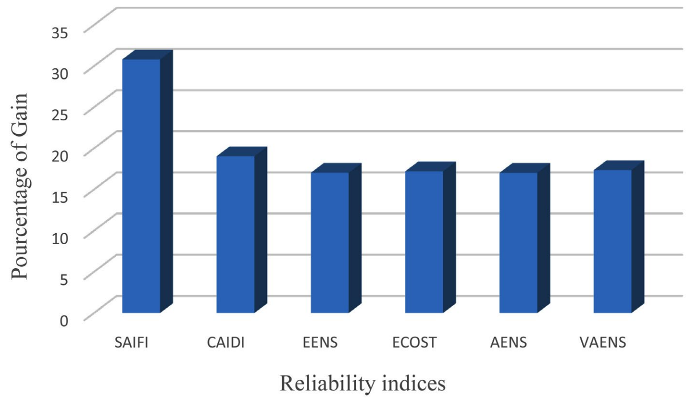

Figure 15. Percentage gain in the improvement of reliability indices for the hybrid distribution network.

It can be observed from Table 7 and Figure 15 above that optimizing the geographical coordinates of photovoltaic production sites yields significant gains across all reliability indices. This indicates that optimizing the geographical coordinates of PV sites relative to a target distribution substation (for power injection) has a positive impact on the reliability index values of an electrical distribution network.

5. Conclusions

To improve the reliability of an electrical distribution network in the context of global warming, the ideal approach is to utilize clean, inexhaustible energy sources (such as photovoltaic generation). This research highlights a novel approach to enhancing distribution network reliability by optimizing the geographical coordinates of actual, distributed photovoltaic production sites. The results obtained 30.80%, 19.03%, 17.03%, 17.20%, and 17.02% for SAIFI, CAIDI, EENS, ECOST, and AENS, respectively, demonstrate the effectiveness of this new reliability improvement method.

However, hybridizing the algorithm proposed in this study, incorporating energy storage systems, and considering potential siting constraints relative to conventional network substations represent promising avenues for future research in this field.

Author Contributions

Moussa Ahmat conceived and designed the study, developed the methodology, formulated the optimization model, implemented the IPSO algorithm, performed the simulations, analyzed the results, and wrote the original manuscript. **Jean Benjamin BIDIAS** contributed to the development of the reliability assessment methodology and supervised the research. **Yacoub Nassian Nimir** contributed to the validation of the results and critically reviewed the manuscript. All authors contributed to the interpretation of the results, reviewed the manuscript, and approved the final version.

Conflicts of Interest

The authors declare no conflicts of interest regarding the publication of this paper.

References

[1] Emmanuel, M. and Rayudu, R. (2017) Evolution of Dispatchable Photovoltaic System Integration with the Electric Power Network for Smart Grid Applications: A Review. *Renewable and Sustainable Energy Reviews*, **67**, 207-224. https://doi.org/10.1016/j.rser.2016.09.010

[2] Cruz, L.M., Alvarez, D.L., Al-Sumaiti, A.S. and Rivera, S. (2020) Load Curtailment Optimization Using the PSO Algorithm for Enhancing the Reliability of Distribution Networks. *Energies*, **13**, Article 3236. https://doi.org/10.3390/en13123236

[3] Vempalle, R. and Dhal, P.K. (2020) Loss Minimization by Reconfiguration along with Distributed Generator Placement at Radial Distribution System with Hybrid Optimization Techniques. *Technology and Economics of Smart Grids and Sustainable Energy*, **5**, Article No. 18. https://doi.org/10.1007/s40866-020-00088-2

[4] Ibrik, I.H. (2020) Techno-Economic Assessment of On-Grid Solar PV System in Palestine. *Cogent Engineering*, **7**, Article 1727131. https://doi.org/10.1080/23311916.2020.1727131

[5] Siewierski, T., Szypowski, M. and Wedzik, A.W. (2018) A Review of Economic Aspects of Voltage Control in LV Smart Grids. *Renewable and Sustainable Energy Reviews*, **88**, 37-45. https://doi.org/10.1016/j.rser.2018.02.013

[6] Saboori, H. and Hemmati, R. (2016) Considering Carbon Capture and Storage in Electricity Generation Expansion Planning. *IEEE Transactions on Sustainable Energy*, **7**, 1371-1378. https://doi.org/10.1109/tste.2016.2547911

[7] Džodić, K., Krstivojević, J., Abarrategi, O. and Eguia, P. (2024) Reliability Enhancement through Optimal Placement of Photovoltaic Power Plant and Battery Energy Storage in Distribution System. *Renewable Energy and Power Quality Journal*, **22**, 39-43. https://doi.org/10.52152/3968

[8] Aliabadi, M.J. and Radmehr, M. (2024) Hybrid Energy System Optimization Integrated with Battery Storage in Radial Distribution Networks Considering Reliability and a Robust Framework. *Scientific Reports*, **14**, Article No. 26597. https://doi.org/10.1038/s41598-024-73808-8

[9] Xiao, J., Ye, Y., Wang, F., Shen, J. and Gao, F. (2022) Comprehensive Evaluation Index System of Distribution Network for Distributed Photovoltaic Access. *Frontiers in Energy Research*, **10**, Article ID: 892579. https://doi.org/10.3389/fenrg.2022.892579

[10] Jain, A. and Gupta, S.C. (2024) Optimal Placement of Distributed Generation in Power Distribution System and Evaluating the Losses and Voltage Using Machine Learning Algorithms. *Frontiers in Energy Research*, **12**, Article ID: 1378242. https://doi.org/10.3389/fenrg.2024.1378242

[11] Sinishaw, G.Y., Bantyirga, B. and Abebe, K. (2021) Analysis of Smart Grid Technology Application for Power Distribution System Reliability Enhancement: A Case Study on Bahir Dar Power Distribution. *Scientific African*, **12**, e00840. https://doi.org/10.1016/j.sciaf.2021.e00840

[12] Jaleel, A. and Abd, M. (2021) Reliability Evaluation of Electric Distribution Network with Distributed Generation Integrated. *International Journal of Intelligent Engineering and Systems*, **14**, 306-319. https://doi.org/10.22266/ijies2021.1031.28

[13] Durgadevi, A. and Shanmugavadivoo, N. (2023) Availability Capacity Evaluation and Reliability Assessment of Integrated Systems Using Metaheuristic Algorithm. *Com-*

puter Systems Science and Engineering, **44**, 1951-1971. https://doi.org/10.32604/csse.2023.026810

[14] Suyono, H., Hasanah, R.N., Mudjirahardjo, P., Purnomo, M.F.E., Uliyani, S., Musirin, I. and Awalin, L.J. (2020) Enhancement of the Power System Distribution Reliability Using ant Colony Optimization and Simulated Annealing Methods. *Indonesian Journal of Electrical Engineering and Computer Science*, **17**, 877-885. https://doi.org/10.11591/ijeecs.v17.i2.pp877-885

[15] Ali Shaik, M., Mareddy, P.L. and N., V. (2022) Enhancement of Voltage Profile in the Distribution System by Reconfiguring with DG Placement Using Equilibrium Optimizer. *Alexandria Engineering Journal*, **61**, 4081-4093. https://doi.org/10.1016/j.aej.2021.09.063

[16] Agajie, T.F., Khan, B., Guerrero, J.M. and Mahela, O.P. (2021) Reliability Enhancement and Voltage Profile Improvement of Distribution Network Using Optimal Capacity Allocation and Placement of Distributed Energy Resources. *Computers & Electrical Engineering*, **93**, Article 107295. https://doi.org/10.1016/j.compeleceng.2021.107295

[17] Sai Kiran, R. and Suresh Reddy, S. (2023) A Mixed Integer Optimization Model for Reliability Indices Enhancement in Micro-Grid System with Renewable Generation and Energy Storage. *Materials Today*: *Proceedings*, **80**, 2937-2944. https://doi.org/10.1016/j.matpr.2021.07.076

[18] Josue, N.O., Li, B., Mahato, N.K. and Jaime, N. (2024) Load Profile Analysis for Mitigating Load-Shedding in Central Africa: Case of Kinshasa. *Journal of Power and Energy Engineering*, **12**, 1-19. https://doi.org/10.4236/jpee.2024.128001

[19] Mansaray, M.O., Diawuo, F.A. and Bantinge, B. (2024) Integration of Multiple Distributed Solar PV (DSP) into the Grid: The Case of the Distribution Network in Freetown, Sierra Leone. *Solar Compass*, **10**, Article 100075. https://doi.org/10.1016/j.solcom.2024.100075

[20] Nicodemus, K., Muriithi, C. and Mambo, S. (2025) Maintaining the Electrical Distribution Grid Network Reliability with Distributed Photovoltaic Generations. *Journal of Energy Systems*, **9**, 116-131. https://doi.org/10.30521/jes.1527231

[21] Taryam, E. (2021) L'accès à l'énergie au tchad: Un frein au développement. https://thinkingafrica.org/lacces-a-lenergie-au-tchad-un-frein-au-developpement/

[22] Melaku, E.D., Bayu, E.S., Roy, C., Ali, A. and Khan, B. (2023) Distribution Network Forecasting and Expansion Planning with Optimal Location and Sizing of Solar Photovoltaic-Based Distributed Generation. *Computers and Electrical Engineering*, **110**, Article 108862. https://doi.org/10.1016/j.compeleceng.2023.108862

[23] Kumar, A., Verma, R., Choudhary, N.K. and Singh, N. (2023) Optimal Placement and Sizing of Distributed Generation in Power Distribution System: A Comprehensive Review. *Energy Sources*, *Part A*: *Recovery*, *Utilization*, *and Environmental Effects*, **45**, 7160-7185. https://doi.org/10.1080/15567036.2023.2216167

[24] Zhang, B. and Gao, Y. (2023) Data-Driven Voltage/Var Optimization Control for Active Distribution Network Considering PV Inverter Reliability. *Electric Power Systems Research*, **224**, Article 109800. https://doi.org/10.1016/j.epsr.2023.109800

[25] Hemakumar Reddy, G., Rani Depuru, S., Bhattacharya, D., Gunaga, S.R., Gope, S. and Nayak Bhukya, M. (2023) (2023) Distribution System Reliability by Considering Operational Failures and Distributed Generation. 2023 *International Conference on Computational Intelligence for Information*, *Security and Communication Applications* (*CIISCA*), Bengaluru, 22-23 June 2023, 76-81. https://doi.org/10.1109/ciisca59740.2023.00025

[26] Kumar, C., Manojkumar, R., Ganguly, S. and Liserre, M. (2021) Impact of Optimal Con-

trol of Distributed Generation Converters in Smart Transformer Based Meshed Hybrid Distribution Network. *IEEE Access*, **9**, 140268-140280.
https://doi.org/10.1109/access.2021.3119349

Appendix

Abbreviations, symbols, terms, and abbreviations used in this study are presented in bellow table (Table A1).

Table A1. Symbols, terms and abbreviations.

Symbols, terms and abbreviations	Significations
MV	Medium Voltage
LV	Low Voltage
SNE	Chad's National Electricity Company
CDN	Conventional Distribution Network
GHG	Greenhouse gases
RES	Renewable Energy Source
SAIFI	System Average Interruption Frequency Index
SAIDI	System Average Interruption Duration Index
CAIDI	Customer Average Interruption Duration Index
EENS	Expected Energy Not Served
ECOST	Cost of Expected Energy Not Supplied
AENS	Average Energy Not Supplied per customer served
VAENS	Average cost of unsupplied energy per customer served
IPSO	Improved Particle Swarm Optimization
Lb	Lower search bound
Ub	Upper search bound
rand	Random number generated within the interval]0, 1[
Pbest	Optimal location of the individual production site
Lbest	Optimal location for the neighboring production site
Gbest	Optimal locations sites for the entire distribution network
V_i^{k+1}	Particle velocities at iterations $k+1$
V_i^k	Particle velocities at iterations k
x_i^{k+1}	Longitude of site i at iterations $k+1$
x_i^k	Longitude of site i at iterations k
y_i^{k+1}	Latitude of site i at iterations $k+1$
y_i^k	Latitude of site i at iterations k
ω	Inertia weight
ω_{max}	Initial weight
ω_{min}	Final weight
$iter$	Current iteration
$itermax$	Maximum number of iterations